

NUMERICAL PREDICTION OF MECHANICAL PROPERTIES OF DUAL-PHASE STEEL BY USING MULTI-PHASE-FIELD METHOD AND HOMOGENIZATION METHOD

A. YAMANAKA^{*} AND T. TAKAKI[†]

^{*} Graduate School of Mechanical and Control Engineering,
Tokyo Institute of Technology
2-12-1, O-okayama, Meguro-ku, Tokyo, 152-8552, Japan
e-mail: ayamanaka@mes.titech.ac.jp

[†] Graduate School of Science and Technology,
Kyoto Institute of Technology
Matsugasaki, Sakyo-ku, Kyoto, 606-8585, Japan
email: takaki@kit.ac.jp

Key words: Mullti-Phase-Field Method, Crystal Plasticity Finite Element Method, Homogenization Method, Dual-Phase Steel, Microstructure.

Abstract. In this study, a numerical prediction method by combining the crystal plasticity finite element method, the multi-phase-field method and the homogenization method is developed to predict microstructure formation and mechanical property of the dual-phase (DP) steel efficiently. With the developed method, the austenite – to – ferrite transformation from the deformed austenite phase is simulated and the mechanical properties of the DP steel which includes the predicted microstructure are investigated.

1 INTRODUCTION

The mechanical property of ferrite (α) + martensite (α') dual-phase (DP) steel is largely characterized by distribution of the microstructure. It is also well-known that the refinement of α grain size by thermo-mechanical controlled processing (TMCP) is quite essential to improve strength of the DP steel. Therefore, to understand the austenite-to-ferrite ($\gamma - \alpha$) transformation behavior in deformed γ phase during the TMCP is quite important to control the mechanical property of the DP steel. However, since the $\gamma - \alpha$ transformation is influenced

by several factors, e.g. chemical composition, transformation temperature, γ grain size and strain applied by the TMCP, it is difficult to predict the transformation behavior only by experiments.

Recently, it has been well-recognized that the multi-phase-field method (MPFM) is a powerful simulation tool to predict microstructure evolutions in polycrystalline materials [1]. The most attractive advantage of the MPFM is to simulate morphological change of microstructures. Therefore, if we utilize digital data of the microstructure morphology simulated by the MPFM as input data for finite element (FE) simulation, systematic simulation model for steel design can be realized [2]. This will enable us to predict the microstructure formation and the mechanical property of the DP steel efficiently.

Therefore, the purpose of this study is to develop a numerical prediction method by combining the crystal plasticity FE method (CPFEM), the MPFM and the homogenization method. In this paper, we simulate the γ - α transformation from the deformed γ phase and evaluate the mechanical properties of the DP steel which includes the predicted microstructure. Then, the effects of the distribution of α phase on macro- and microscopic deformation behavior of the DP steel are studied.

2 SIMULATION METHOD

The procedures to simulate the γ - α transformation from the deformed γ phase and evaluate the mechanical property of the DP steel are as follows: First, to simulate the hot plastic forming of Fe-C alloy, simulation of compression deformation of polycrystalline γ phase is conducted by the CPFEM based on the strain gradient crystal plasticity theory. Second, nucleation rate and nucleation site of the α phase in the deformed γ phase are estimated based on the classical nucleation theory. Third, the γ - α transformation during continuous cooling process is simulated by the MPFM with the estimated nucleation condition. Finally, we perform numerical simulation of uniaxial tensile test of the DP steel by the CPFEM based on the homogenization method with the simulated microstructure.

2.1 Strain gradient crystal plasticity theory

In order to simulate plastic deformation behavior of polycrystalline γ phase during the hot plastic forming, we employ the following crystal plasticity constitutive equation [3],

$$\overset{\nabla}{S}_{ij} = D_{ijkl}^e \varepsilon_{kl} - \sum_{\alpha=1}^2 \left(D_{ijkl}^e P_{kl}^{(\alpha)} + W_{ik}^{(\alpha)} \sigma_{kj} + \sigma_{ik} W_{kj}^{(\alpha)} \right) \dot{\gamma}^{(\alpha)} \quad (1)$$

Here, $\overset{\nabla}{S}_{ij}$, D_{ijkl}^e , ε_{ij} , σ_{ij} and $\dot{\gamma}^{(\alpha)}$ are the Jaumann rate of Kirchoff stress tensor, the elastic modulus tensor, the strain tensor, the Cauchy stress tensor and the plastic shear strain rate on the slip system α , respectively. Also, $P_{ij}^{(\alpha)}$ and $W_{ij}^{(\alpha)}$ are the schmid tensor and the plastic spin tensor, respectively.

Since we use the strain rate dependent crystal plasticity constitutive equation [4], the plastic shear strain rate is defined as follows:

$$\dot{\gamma}^{(\alpha)} = \dot{\gamma}_0^{(\alpha)} \frac{\tau^{(\alpha)}}{g^{(\alpha)}} \left(\frac{\tau^{(\alpha)}}{g^{(\alpha)}} \right)^{\frac{1}{m}-1} \quad (2)$$

where $\dot{\gamma}_0^{(\alpha)}$ is the reference shear strain rate and the resolved shear stress $\tau^{(\alpha)}$ is calculated by $\tau^{(\alpha)} = \sum_{\alpha=1}^2 P_{ij}^{(\alpha)} \sigma_{ij}$. The evolution equation of the critical resolved shear stress (CRSS) $g^{(\alpha)}$ is chosen as,

$$g^{(\alpha)} = g_0^{(\alpha)} + a\mu\tilde{b} \sum_{\beta=1}^2 \omega_{\alpha\beta} \sqrt{\rho_a^{(\alpha)}} \quad (3)$$

Here, $g_0^{(\alpha)}$, a , μ , \tilde{b} and $\omega_{\alpha\beta}$ are the initial critical resolved shear stress, the shear elastic modulus, the magnitude of burgers vector and the dislocation interaction coefficient, respectively. The accumulated dislocation density is given as follows:

$$\rho_a^{(\alpha)} = \rho_{SS}^{(\alpha)} + \|\rho_{GN}^{(\alpha)}\| \quad (4)$$

where $\rho_{SS}^{(\alpha)}$ and $\rho_{GN}^{(\alpha)}$ are the statically stored dislocation (SSD) density and the geometrically necessary dislocation (GND) density, respectively. In this study, the following evolution equation for the SSD density is used.

$$\dot{\rho}_{SS}^{(\alpha)} = \frac{c|\dot{\gamma}^{(\alpha)}|}{\tilde{b} \sqrt{\sum_{\beta=1}^2 \omega_{\alpha\beta} (\rho_{SS}^{(\alpha)} + \|\rho_{GN}^{(\alpha)}\|)}} \quad (5)$$

And, the GND density is evaluated as,

$$\|\rho_{GN}^{(\alpha)}\| = \sqrt{\left(-\frac{1}{\tilde{b}} \frac{\partial \gamma^{(\alpha)}}{\partial x_i} s_i^{(\alpha)} \right)^2 + \left(\frac{1}{\tilde{b}} \frac{\partial \gamma^{(\alpha)}}{\partial x_i} e_{ijk} s_j^{(\alpha)} m_k^{(\alpha)} \right)^2} \quad (6)$$

where $\rho_{GN,edge}^{(\alpha)}$ and $\rho_{GN,screw}^{(\alpha)}$ are the edge and screw components of the GND density, respectively. With the accumulated dislocation density ρ_a , the stored energy E_{store} can be derived as

$$E_{store} = \frac{1}{2} \mu \tilde{b}^2 \sum_{\alpha=1}^2 \rho_a^{(\alpha)} \quad (7)$$

2.2 Modeling of α nucleation behavior

In this study, the potential nucleation sites (i.e., grain boundary corner, grain boundary edge, grain boundary face and deformation band) and the nucleation rate at each nucleation site are estimated by using the results of the hot plastic forming simulation.

According to the classical nucleation theory, the nucleation rate of α phase J^i is described as,

$$J^i(C_\gamma, T, t) = d^i(t) \beta^* Z \exp\left(-\frac{1}{kT} \frac{\Psi^i}{\Delta G_\gamma^2(C_\gamma, T)}\right) \quad (8)$$

where $d^i(t)$ is density of the potential nucleation site, where upper subscription i means kind of the above mentioned nucleation sites ($i = c, e, f$ and d). Since the nucleation site is consumed with progression of the transformation, $d^i(t)$ is defined as a function of time t . β^* is the frequency coefficient which is assumed to be related to the temperature-dependent carbon diffusion coefficient in the γ phase as $\beta^* = \lambda D_\gamma(T)$. Z , k , T and C_γ are the Zeldovich parameter, the Boltzmann constant, the temperature of the system and the carbon concentration in the γ phase, respectively. Also, Ψ^i is the geometry coefficient of nucleation site i . The chemical driving force for the nucleation $\Delta G_\gamma(C_\gamma, T)$ can be calculated based on the CALPHAD method.

The density of the potential nucleation site $d^i(t)$ in Eqn.(8) is calculated by $d^i(t) = N^i(t) / S$ where $N^i(t)$ and S are number of potential nucleation site and area of the system, respectively. $N^i(t)$ is determined using the number of grain n which is explained in next section and the misorientation $\Delta\theta$. That is, a computational grid satisfying $n = 4$ is considered as a potential nucleation site on the grain boundary corner. Similarly, position of the potential nucleation sites on the grain boundary edge ($n = 3$) and the grain boundary face ($n = 2$) is determined. For the nucleation sites in the deformation band, we assume that high-angle grain boundary region which is given as $n = 1$ and $\Delta\theta > 15^\circ$ or the region in which the stored energy E_{store} is more than a critical value E_{cri} is possible site. As a result, time interval for the α nucleation at each nucleation site is given by inverse of Eqn. (8). For all nucleation sites, order of the α nucleation is determined by order of the magnitude of the stored energy.

2.3 Multi-Phase-Field method

The γ - α transformation during the continuous cooling is simulated by the generalized MPFM proposed by Steinbach et al [5]. In the MPFM, the total free energy of the system, G , is defined as the Ginzburg-Landau free energy functional which is given by the sum of the gradient energy, potential energy and bulk free energy as,

$$G = \int_V \left\{ \sum_{i=1}^N \sum_{k=i+1}^N \left(-\frac{a_{ik}^2}{2} \nabla \phi_i \cdot \nabla \phi_k \right) + \sum_{i=1}^N \sum_{k=i+1}^N (W_{ik} \phi_i \phi_k) + g_{bulk} \right\} dV \quad (9)$$

Here, we use N phase field variables, ϕ_i ($i = 1, 2, 3, \dots, N$). ϕ_i describes the fraction of the i th grain. The phase field variables vary smoothly across the interface from $\phi_i = 1$ in the i th grain to $\phi_i = 0$ in other grain. All phase field variables satisfy the constant, $\sum_{i=1}^N \phi_i = 1$ at all points. a_{ij} and W_{ij} are the gradient coefficient and potential height, respectively. These parameters are related to the interfacial energy and interfacial thickness.

By assuming the total free energy decreases monotonically with time, the evolution equation of the phase field variable is written as,

$$\frac{\partial \phi_j^i}{\partial t} = -\frac{2}{n} \sum_{k=1}^n M_{ik}^\phi \left[\sum_{l=1}^n \left\{ (W_{il} - W_{kl}) \phi_j^l + \frac{1}{2} (a_{il} - a_{kl}) \nabla^2 \phi_j^l \right\} - \frac{8}{\pi} \sqrt{\phi_j^i \phi_j^k} \Delta E_{ik} \right] \quad (10)$$

where n is the number of phase fields in the arbitrary point and is given by $n = \sum_{i=1}^N \xi_i$. Here, ξ_i is a following step function, which is expressed as $\xi_i = 1$ in a region $0 < \phi_i \leq 1$ and $\xi_i = 0$ in other region. The magnitude of the transformation driving force, ΔE_{ij} , is given by sum of the reduction of the chemical free energy and the stored energy obtained by the CPFEM simulation as $\Delta E_{ij} = \Delta E_{chem} + E_{store}$. The chemical driving force is described as $\Delta E_{chem} = \Delta S \Delta T$ at the α - γ interface, where ΔS and ΔT are the entropy difference between the α and γ grains and the undercooling, respectively.

To simulate the diffusion of carbon atoms during γ - α transformation, the total carbon concentration C is defined as a linear function of the local carbon concentration c_i weighted by the phase-field variables ϕ_i . The local carbon concentration is given by the $c_i = k_i c_i / \left(\sum_{j=1}^n k_j \phi_j \right)$. Here, k_i is the partition coefficient of carbon atoms. Hereafter, we consider an $\alpha + \gamma$ two-grain system ($N = 2$) for simple description. Therefore, when ϕ_1 and ϕ_2 correspond to the α and γ phases, respectively.

The diffusion equation for total carbon concentration is expressed by the sum of diffusion fluxes of carbon atoms in the i th grains J_i as,

$$\frac{\partial C}{\partial t} = \nabla \cdot \left\{ \sum_i \phi_i J_i \right\} = \nabla \cdot \left\{ \sum_i \phi_i D_i \nabla C_i \right\} = \nabla \cdot \{ \phi_1 D_1 \nabla c_1 + \phi_2 D_2 \nabla c_2 \} \quad (11)$$

Here, D_i is diffusion coefficient of carbon atom in the i the grain.

In this study, the undercooling ΔT and the partition coefficient k_i are evaluated by using a linearized phase diagram of Fe-C alloy.

2.4 Homogenization method

In this study, we employ the homogenization method proposed by Grudes et al to investigate the mechanical properties of the DP steel which contains the simulated α phase. By using the homogenization method, the micro- and macroscopic deformation behaviors of the steel depending on heterogeneous microstructure morphology can be simulated.

In the homogenization method, we consider the two-scale boundary value problem for the micro- and macroscopic scales as shown in Fig.1. The microstructure in the steel is assumed to be a periodic array of representative volume elements (RVEs). In this study, The RVE describes heterogeneous distribution of the microstructure obtained by the MPFM. x_i and y_i ($i = 1$ and 2) are macro- and microscopic coordinates, respectively. These scales are related to each other as $y_i = x_i / \eta$ with a parameter η . By using these two coordinates, the velocity can be described by the following asymptotic expansion with η :

$$\dot{u}_i(x, y) = \eta^0 \dot{u}_i^0(x, y) + \eta \dot{u}_i^1(x, y) + \eta^2 \dot{u}_i^2(x, y) + \dots \quad (12)$$

Here, we use the first order approximation as,

$$\dot{u}_i(x, y) = \dot{u}_i^0(x) + \eta \dot{u}_i^1(x, y) = \dot{u}_i^0(x) + \eta \left(-\chi_i^{mn} \frac{\partial \dot{u}_m^0}{\partial x_n} + \phi \right) \quad (13)$$

where $\dot{u}_i^0(x, y)$ represents the homogenized macroscopic velocity. χ_i^{mn} and ϕ_i are the characteristic velocities which corresponds to components of macro-velocity gradient tensor, respectively. With Eqns.(12) and (13), the velocity gradient L_{ij} is given by,

$$L_{ij}(x, y) = \frac{\partial \dot{u}_i(x, y)}{\partial x_j} = \frac{\partial \dot{u}_i^0(x)}{\partial x_j} + \frac{\partial \dot{u}_i^1(x, y)}{\partial y_j} = \frac{\partial \dot{u}_i^0(x)}{\partial x_j} - \frac{\partial \chi_i^{mn}}{\partial y_j} \frac{\partial \dot{u}_m^0(x)}{\partial x_n} + \frac{\partial \phi_i(x)}{\partial y_j} \quad (14)$$

According to the updated Lagrange formulation and the strain gradient crystal plasticity theory explained in previous section, the principle of virtual work is written as,

$$\int_{\Omega} (C_{ijkl} - H_{ijkl}) L_{kl} \delta L_{ij} dV = \int_S \dot{P}_i \delta u_i dS + \int_V \sum_{a=1}^2 R_{ij}^{(a)} \dot{f}^{(a)} \delta L_{ij} dV \quad (15)$$

To accomplish the homogenization formulation, we take the limit of η to zero and employing the following integral formula,

$$\lim_{\eta \rightarrow 0} \int_{\Omega} \Phi \left(x, y = \frac{x}{\eta} \right) d\Omega = \frac{1}{|Y|} \int_{\Omega} \int_Y \Phi \left(x, y = \frac{x}{\eta} \right) dY d\Omega \quad (16)$$

where is Φ a so-called Y -periodic function. The integral sing $\frac{1}{|Y|} \int_Y \Phi(x, y) dY$ means the volume average of function Φ in a RVE. By substituting Eqn. (14) into Eqn.(15) and introduce Eqn.(16), we can derive the governing equations for the macro- and microscopic regions, respectively.

$$\int_{\Omega} \frac{1}{|Y|} \int_Y C'_{ijkl} \left(\frac{\partial \dot{u}_k^0}{\partial x_l} + \frac{\partial \dot{u}_l^1}{\partial y_k} \right) \frac{\partial \delta \dot{u}_k^0}{\partial x_l} dY d\Omega = \int_S \dot{P}_i \delta \dot{u}_i^0 dS + \frac{1}{|Y|} \int_{\Omega} \int_Y \sum_{a=1}^2 R_{ij}^{(a)} \dot{f}^{(a)} \frac{\partial \delta \dot{u}_k^0}{\partial x_l} dY d\Omega \quad (17)$$

$$\int_{\Omega} \frac{1}{|Y|} \int_Y C'_{ijkl} \left(\frac{\partial \dot{u}_k^0}{\partial x_l} + \frac{\partial \dot{u}_l^1}{\partial y_k} \right) \frac{\partial \delta \dot{u}_l^1}{\partial y_k} dY d\Omega = \frac{1}{|Y|} \int_{\Omega} \int_Y \sum_{a=1}^2 R_{ij}^{(a)} \dot{f}^{(a)} \frac{\partial \delta \dot{u}_l^1}{\partial y_k} dY d\Omega \quad (18)$$

Since we obtain the velocity of displacement in the micro- and macro scale by solving Eqns.(17) and (18) with the finite element method, the variation of strain and stress in the steel can be calculated.

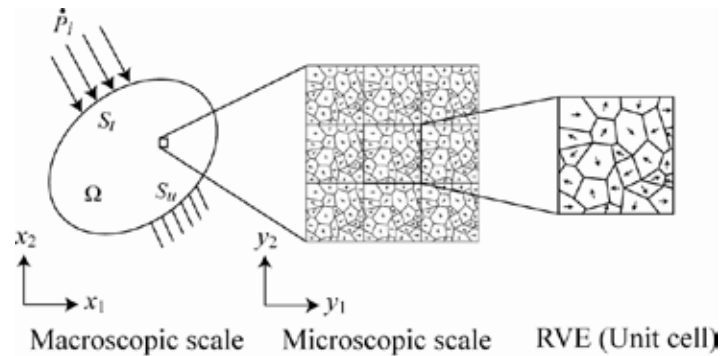


Figure 1: Schematic explanation of two-scale boundary value problem

3 SIMULATION RESULTS

Figure 2 shows the simulation model used in the hot plastic forming simulation. The computational region is meshed with 128 x 128 crossed-triangle elements. The size of a finite

element is set to be $\Delta X = \Delta Y = 0.5 \mu\text{m}$. Since a two-slip system is assumed for simplicity, the crystal orientation is defined by the rotation angle θ as shown in Fig.2(b). The initial polycrystalline structure of the γ phase consists twenty grains with random crystal orientations. These γ grains are compressed up to strain of $\varepsilon = 0.2$ at a strain rate of 10^{-3} s^{-1} . In this study, we assume the plain strain problem and the periodic boundary condition. The temperature is assumed to be 1150 K which is lower than the recrystallization temperature of steels, 1173 K.

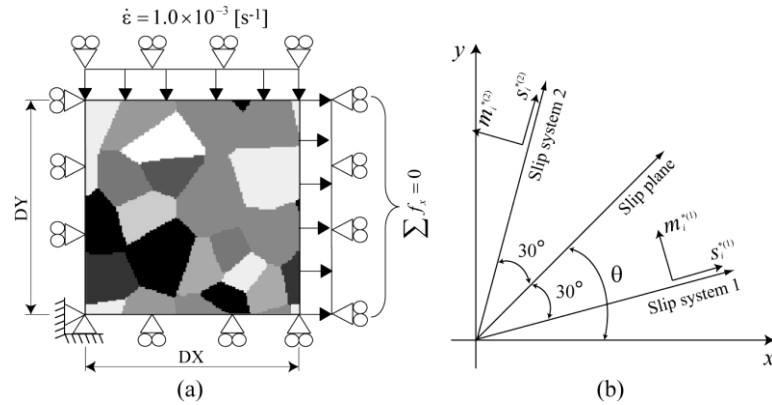


Figure 2: Simulation model for compression deformation of polycrystalline γ phase and definition of crystal orientation θ in a two-slip system

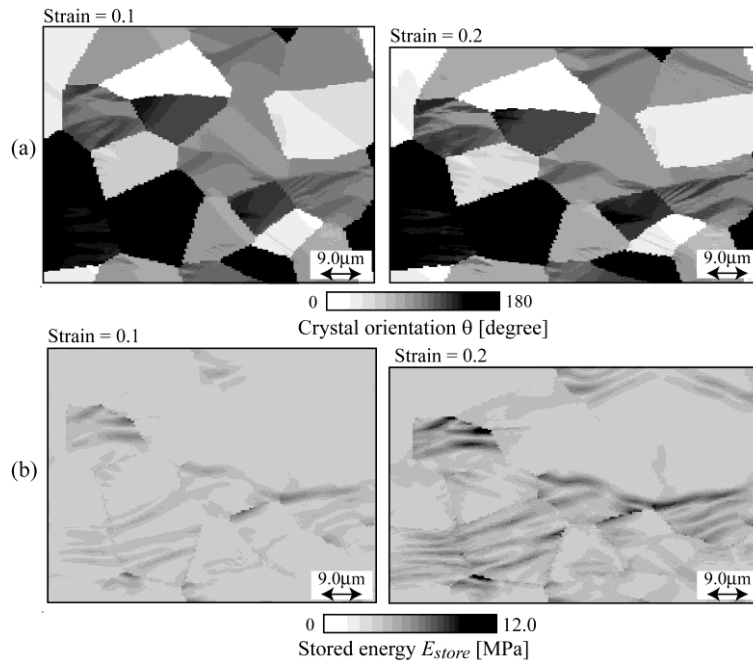


Figure 3: Distributions of (a) crystal orientation and (b) stored energy in deformed γ phase

Table 1: Parameters for α nucleation

Geometry coefficient, ϕ^c	$1.30 \times 10^{-6} [\text{J}^3/\text{m}^6]$
Geometry coefficient, ϕ^e	$5.00 \times 10^{-8} [\text{J}^3/\text{m}^6]$
Geometry coefficient, ϕ^f and ϕ^g	$2.10 \times 10^{-6} [\text{J}^3/\text{m}^6]$
Zeldovich constant, Z	0.05
Parameter, λ	75

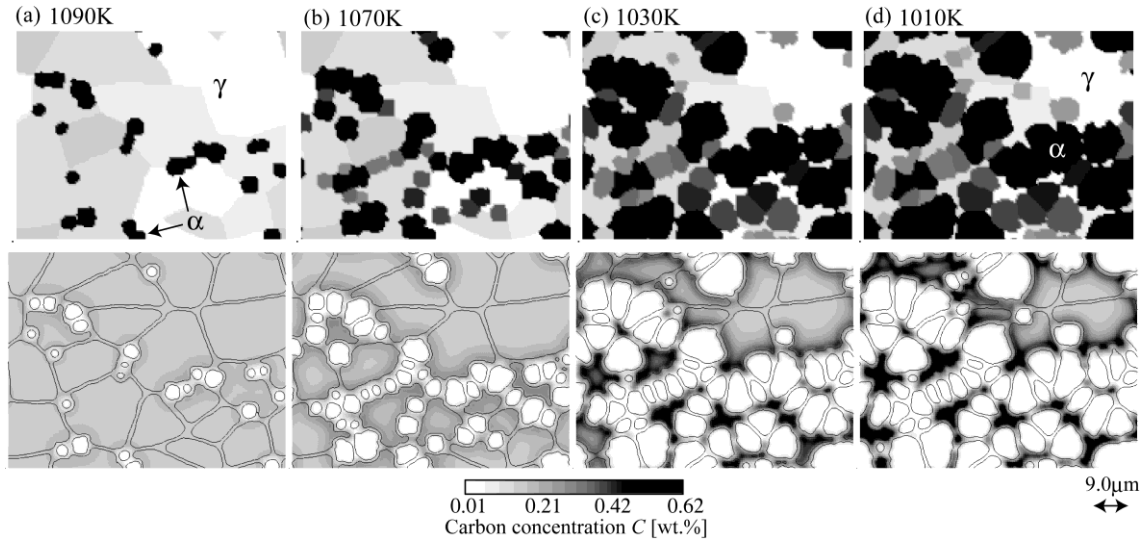
**Figure 4:** Distributions of (a) α and γ grains and (b) carbon concentration during γ -to- α transformation

Figure 3 shows the distributions of crystal orientation and stored energy in the deformed γ phase at different strains. As shown in Fig.3(b), the stored energy is increased with the increasing strain. In particular, the strain energy tends to concentrate near grain boundaries, because dislocations accumulate at the grain boundary. On the other hand, it is found that the region which exhibits high strain energy and large crystal rotation is formed with in some γ grain interiors. This indicates the deformation band is introduced in the γ phase by the plastic forming. Also, it is clearly shown that large crystal rotation is occurred in the deformed γ phase.

Based on the simulated deformed γ phase, the γ - α transformation is simulated. The distributions of crystal orientation and stored energy shown in Fig.3 are mapped on the computational region for the MPF simulation. The initial temperature and initial carbon concentration of γ phase are set to be 1110 K and 0.2 wt%, respectively. The parameters for the α nucleation are summarized in Table 1. The computational region is meshed with 144×112 finite difference grid. The size of the grid is set to be $\Delta x = \Delta y = 0.5 \mu\text{m}$. In this simulation,

Table 2: Material parameters for uniaxial tensile test

Elastic constants, C_{11}, C_{12}, C_{44}	$C_{11} = 237$ [GPa] $C_{12} = 141$ [GPa] $C_{44} = 116$ [GPa]
Poisson's ratio, ν	0.345
Reference shear strain, $\dot{\gamma}_0^{(\alpha)}$	0.001 [1/s]
Initial CRSS, $\tau_0^{(\alpha)}$	200 [MPa] (α phase) 380 [MPa] (α' phase)
Strain rate sensitivity constant, $1/m$	0.05
Parameter, a	0.4
Shear modulus, μ	80.7 [GPa]
Length of burgers vector, \tilde{b}	0.2624 [nm]
Initial dislocation density, ρ_0	10^{-10} [1/m]
Dislocation interaction matrix, ω_{ij}	1.0 (all componets)

we assume the critical value of stored energy E_{cri} for the α nucleation to be $E_{cri} = 15$ MPa, because it is difficult to determine this value from experiments.

Figure 4 shows the evolutions of α and γ grains and the variation of carbon concentration during γ - α transformation. The temperature is decreased from 1110 K to 1010 K with cooling rate of $\Delta T = 5$ K/s. We can see that inhomogeneous nucleation of α phase is occurred during the continuous cooling. At 1090 K, it is found that some α grains are newly formed and these α grains tend to locate at grain boundary corner and edge. With decreasing temperature due to the cooling, more α grains are nucleated on the grain boundary face and the grain interior. According to the distribution of α phase at 1010 K, it is demonstrated that the formation of α phase is concentrated on the grain boundary of the γ grains with large stored energy.

The uniaxial tensile test of the DP steel is conducted with the CPFEM based on the homogenization method. In this study, the RVE is modeled with the simulated microstructure shown in Fig.4(d). Here, the untransformed γ phase after the continuous cooling is assumed to be transformed into uniform α' phase by quenching to room temperature. Size of the RVE is same as that of the computational domain for the MPFM simulation. In the tensile test, the system is deformed up to a true strain of 0.1 at a strain rate of 10^{-4} s⁻¹. Although the crystal structure of α and α' phases is body-centered cubic, we consider only 12 slip systems on $\{110\}$ plane along $\langle 111 \rangle$ direction for simplicity. The material parameters and physical values for α and α' phases are listed in Table 2.

Figure 5 indicates the calculated macroscopic stress-strain (SS) curve of the DP steel. Similar to the experimental results, the obtained SS curve exhibits continuous yielding behavior and high strain hardening behavior.

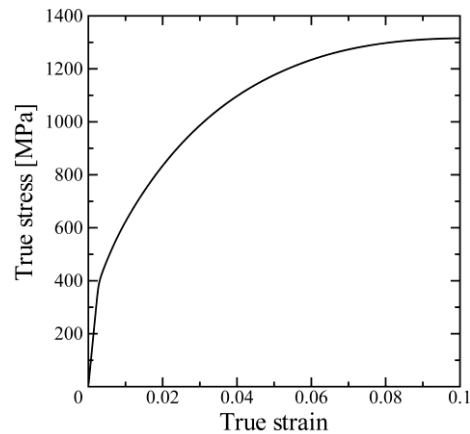


Figure 5: Macroscopic stress-strain curve of the DP steel

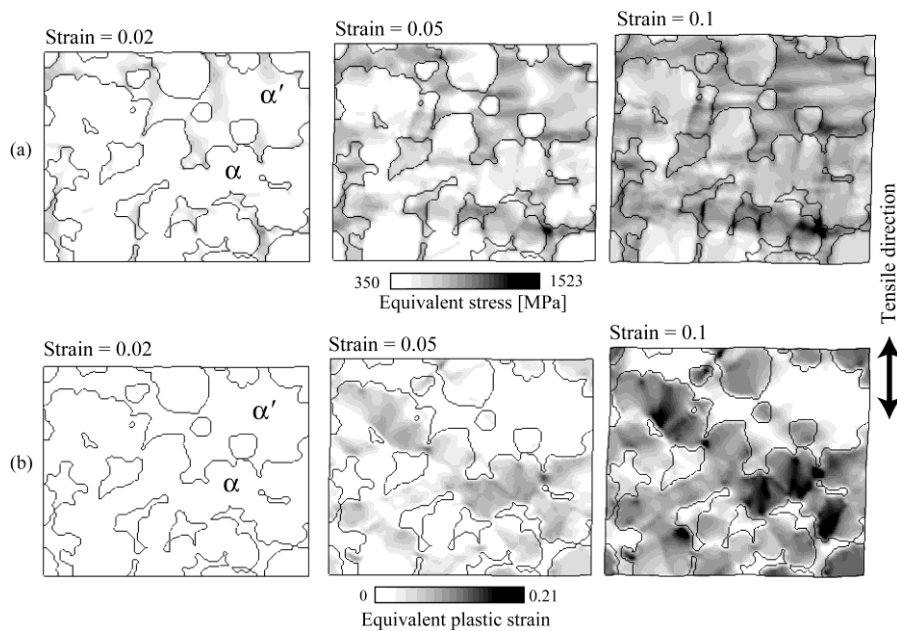


Figure 6: Distributions of (a) equivalent stress and (b) equivalent plastic strain for different strains

In this study, since we employ the homogenization method, not only the macroscopic mechanical response, but also the microscopic deformation behavior of the DP steel can be investigated. Figure 6 shows the distributions of the equivalent stress and equivalent plastic strain in the DP microstructure at different macroscopic strains ($\varepsilon = 0.02, 0.05$ and 0.10), respectively. As shown in Fig.6(a), the stress is increased with increasing macroscopic strain and concentrated in the harder α' phase near the α/α' interface. On the other hand, the plastic strain is generated along the aggregated softer α phase. The simulation results confirm that

the stress concentration at the α' phase is main mechanism of high strength and high strain hardening behavior of the DP steel.

4 CONCLUSIONS

- A numerical prediction method by combining the crystal plasticity finite element method, the multi-phase-field and the homogenization method is developed to predict the microstructure formation and the mechanical property of the DP steel efficiently.
- With a developed method, the γ - α transformation from the deformed γ phase is simulated by the MPFM and the uniaxial tensile test of the DP steel by the CPFEM based on the homogenization method with the simulated microstructure
- Through numerical simulations, the effects of the distribution of α phase on macro- and microscopic deformation behavior of the DP steel which includes the predicted microstructure are clarified.

REFERENCES

- [1] A. Yamanaka, T. Takaki and Y. Tomita, Multi-phase-field modeling of diffusional solid phase transformation in carbon steel during continuous cooling transformation, *Mater. Sci. Eng. A* (2008) **310**: 1337-1342.
- [2] A. Yamanaka, T. Takaki and Y. Tomita, Coupled simulation of microstructural formation and deformation behavior of ferrite-pearlite steel by phase-field method and homogenization method, *Mater. Sci. Eng. A* (2008) **480**: 244-252.
- [3] J. Pan and J. R. Rive, Rate sensitivity of plastic flow and implications for yield-surface vertices, *Int. J. Solid. Struct.* (1983) **19**: 973-987.
- [4] T. Ohashi, Numerical modeling of plastic multislip in metal crystals of f.c.c type, *Philos. Mag. A* (1994) **70**: 793-803.
- [5] I. Steinbach and F. Pezzolla, A generalized field method for multiphase transformation using interface fields, *Physica D* (1999) **134**: 385-393.